Antibacterial Activity of Magnesium Oxide Nanoparticles Against XDR Pseudomonas Aeruginosa Isolated from Burn Infection.

Shareef Saleh Al-khateeb[1], Nawfal Hussein Aldujaili[2]
[1, 2] Kufa University, faculty of science, Department of biology, Iraq
Email: Njjn629@gmail.com

Abstract
This study was intended to study the biological activity of magnesium oxide against XDR *P. aeruginosa* isolated from burns infection. Seventy-Five samples and inquiries were carried out between August 2022 and December 2022. Burn infection samples were obtained from two separate hospitals in the province of Najaf (AL Hakeem hospital and Central Laboratory in najaf). Isolates were identified based on the morphological and microscopic examination, and VITEC. The results showed bacilli were the most common *P. aeruginosa* (52%) followed by *Klebsiella pneumoniae* that the most common Gram-positive was *S. aureus* (20%), while Gram-negative (12%), *Escherichia coli* (8%) , *Burkholderia cepacia* (4%), *Acinetobacter baumannii (2.67%)* and other in (1.33%). Molecular study used ERIC-PCR for the detection of phylogenetic diversity of *P. aeruginosa* isolated from burned samples, In general, 20 isolates characterized using the ERIC molecular techniques had number of bands with some degree of polymorphism using conventional PCR. one efficient isolate (S 10) was selected from screening different strains (36) of probiotics based on antibacterial activity. Isolate S10 was identified as *Lactobacillus acidophilus* depending on morphology, microscopic examination, and VITEK. The study showed the inhibitory ability of *L. acidophilus* all teste isolate showed high anti-biofilm activity against *P.aeruginosa* studied bacteria.
Keywords: Nanotechnology , Magnesium oxide Nanoparticle , XDR P. aeruginosa

1. Introduction

There are many antibiotic-resistant bacteria in burns, and they pose a future threat to patients' lives. The research aims to use nano materials as an alternative or auxiliary to the action of antibiotics. Antimicrobial-resistant (AMR) infections are caused by a microbe that is resistant to an antimicrobial agent. Many disease-fighting drugs lose their effectiveness microbes evolve resistance (1,24). AMR infections kill over 700,000 people per year across the world. By 2050 up to million people a year could die of antimicrobial resistance.(2,25). Magnesium oxide nanoparticles are odorless and nontoxic white powder which possesses high melting point and high hardness. These nanoparticles are widely used in industries due to their biocompatibility, biodegradability, and relatively low cost. In medicine, magnesium oxide is used to relieve heartburn and sour stomach, improve bone regeneration and also as an antimicrobial and antitumor agent (3). Magnesium oxide nanoparticles can be used as effective antimicrobials alone or in combination with other antimicrobial agents (4). Magnesium oxide nanoparticle (MgO) is a light metal based antimicrobial nanoparticle that can be metabolized and fully resorbed in the body. To take advantage of the antimicrobial properties of MgO for medical use, it is necessary to determine the minimal inhibitory, bactericidal and fungicidal concentrations (MIC, MBC and MFC) of MgO against prevalent infectious bacteria and yeasts(5,25). The characterization of biogenic Mgo NPs was achieved, using UV visible spectrophotometry, Field Emission Scanning electron microscope (FESEM), Energy dispersive spectroscopy (EDS), X-ray diffraction (XRD), and atomic force microscope (AFM). Aim of study Therapeutic effect of biosynthesized Magnesium oxide nanoparticle against pathogen isolated from wound burn.

2. 2. Materials and Methods

Isolation and identification of bacteria from burn infection

Various types of bacteria were isolated (75 isolates) from burns during the period from August 2022 to December 2022 and diagnosed based on morphology, microscopic examination, biochemical test , and VITEK2 compact system.(26).

Selection the efficient isolate that producing Mgo NPs

thirty-six of isolates from different strains were grown in brain heart infusion broth for 24 hours at 37C0. After incubation, add the Magnesium nitrate Mg $(No3)_2$, and then were incubated for 24-hour at 37°C in a shaking incubator at 150 rpm after it the colloidal suspension was centrifuged at 10,000 rpm for 15 minutes, the precipitate was separated, and the precipitate was applied to the industrial Mgo . All isolates (S1-S36) were screened against *E. coli and Staphylococcus aureus* using the Muller Hinton agar well diffusion assay and incubated for 24 hours at 37°C. An efficient isolate (S10) was selected based on color change and antimicrobial activity, be a white

doi.org/10.31838/hiv23.02.134 Reaceived: 15.10.22, Revised: 19.11.22, Accepted: 08.12.22.

precipitate. efficient isolate (S10) was identified as *L. acidophilus* based on morphological, biochemical and Vitec.(26).

Characterization of biosynthesized Magnesium oxide nanoparticles

The physical Characteristic of biosynthesis nanoparticles were characterized by XRD, UV visible, FESEM and AFM .

UV visible spectroscopy

Detection of the Mgo nanoparticles formation was estimated with UV-visible spectroscopy (shimadzu UV-visible 1800 spectrophotometer research laboratory of imam Ali Holy Shrine .

Field Emission Scanning Electron Microscopy (FESEM) analysis

Magnesium oxide nanoparticles were examined at the university of Tehran's electron microscopy unite

Energy dispersive X-Ray spectroscopy (EDS) analysis

At the of university of Tehran, Energy dispersive X-Ray spectroscopy (EDS) was used to perform an elemental analysis of Mgo NPs.

Atomic Force Microscope AFM

AFM was used to estimate the size of Mgo NPs in university of Tehran .

X-ray Diffraction (XRD) Analysis

The X-ray diffraction is used for characterization of Mg NPs in Tehran university.

Antibacterial Activity of Mgo NPs

The antibacterial activities of Mgo NPs were tested with different concentration against Extensively drug-Resistant (XDR) bacteria: Gram-negative (P. aeruginosa) isolated from burn infection, bacteria using diffusion method . With 100µl of bacterial suspension, the agar plate was incubated. using a sterile cork Porer, Pores (7 mm diameter) were created and filled with Mgo NPs (100ul) . After that, First, Petri dish were kept at 4 °C for 2h , then incubated at 37°C for 24 hours antibacterial activities was evaluated and the values were provided an means of triplicate by measuring te growth inhibition zone diameter in millimeters.

Ant- biofilm effect by Mgo nanoparticles

In vitro ant biofilm activity was measured using the 96-well microtiter plate technique. The first well microtiter plate filled with 100 µL BHIB broth medium containing 1% glucose and 100 µL of biogenic Mgo NPs then they were made at several diluted concentrations (512,256,128,64,32,16,8,4 and 2 µg/ml), after that we add in each well microtiter plate 100 µL of the diluted concentration till the last one used as a control to confirm the development of biofilm by bacteria and the inhibition of biofilm formation by Mgo NPs.

Antioxidant activity of Mgo nanoparticles

The DPPH solution (0.006 % w/v) was prepared in 95 percent methanol. Freshly prepared DPPH solution was placed in test tubes, and chitosan NPs (100, 200, 300, 400 ug/ml) were applied to each test tube until the final volume was 2 ml, and discoloration was calculated at 517 nm after 30 minutes in the dark incubation (UV visible spectrophotometer). Measurements were implemented at least in triplicate.

DPPH solution was used as a control which contained the same volume (without chitosan NPs) and 95% methanol was used as the blank. The percentage of DPPH free radical scavenging was calculated using the following equation: DPPH scavenging impact (%) = (Ao –A1) / Ao X 100 where Ao was the absorbance of the control and A1 was the absorbance in the presence of the chitosan. The real absorption decrease caused by test compounds was compared with the positive controls (6).

3. 3. Results and Discussion

Isolation and identification of Bacteria from burn infections

Seventy-five samples were collected from burns infections. The patients who attending to (AL-Hakeem hospital and the Central Laboratory in najaf). Among the 75 isolates, gram positive cocci, *Staphylococcus aureus* 15(20%) was the predominant and the most common gram-negative bacilli were *Pseudomonas aeruginosa* 39 (52%) followed by *Klebsiella pneumonia* 9 (12%), *Escherichia coli* 6 (8%), *B.cepacia* 3(4%), *A.baumannii* 2(2.67%) and others 1 (1.33%) Figure (3-1).

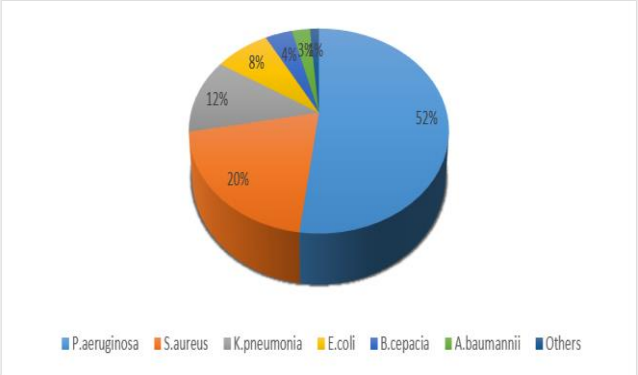

Figure (3-1): Bacterial percentage among clinical samples.

Selection the efficient isolate that producing Mgo NPs

Thirty-six isolates from various sources (S1-S36) were tested against *P. aeruginosa* as an indicator strain for Mgo Nanoparticle production. The most effective isolate was chosen based on the formation of a white precipitate (Figure 3-2) (7), UV spectrum And the biological activity of Mgo nanoparticles in against *P. aeruginosa* . S10 *(Lactobacillus acidophilus*) was the most effective isolate.

Because each microbe has a unique metabolic process and enzyme activity, not all bacteria can manufacture nanoparticles (8).

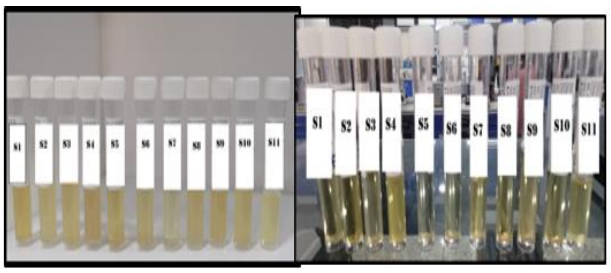

Figure (3-2): Selection of efficient strain S10 (L. acidophilus) Based on the formation of white precipitate and antibacterial activities. A: Before production Mgo. B: After production Mg

This method was chosen because of the advantages of external synthesizing over intracellular biosynthesis. Extracellular biosynthesis has several advantages, including a more straightforward, less artefact-prone approach (9). Nanobiosynthesis isn't possible in all organisms. The exact mechanisms that lead to the creation of biogenic Mgo NPs have yet to be determined. Mgo NPs are produced biologically as nanoparticles with a size of less than 100nm. As. The Lactobacillus strain has been widely employed in the industry due to its ability to produce amylase, alkaline, protease, keratinase, and manganese (10).

UV-visible Spectroscopy

UV- Visible spectrophotometric is a proven technique for detecting the nanoparticles. After 24 hours of incubation of the reaction mixture, colour change was observed which indicated the formation nanoparticles in the reaction mixture. The biosynthesis of nanoparticles can be confirmed by visual observation and measuring the absorbance band using UV-visible spectroscopy. The absorption spectrum of nanoparticles produced in the reaction mixture has a peak at 280nm figure (3-3).

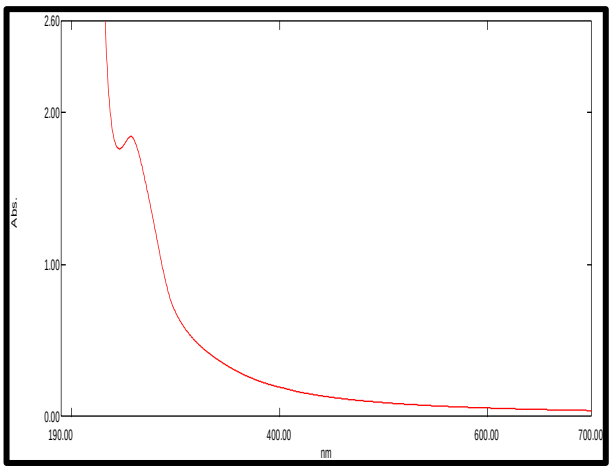

Figure (3-3) UV-visible spectroscopy analysis of Mgo NPs synthesis by L. acidophilus

Field Emission Scanning Electron Microscopy (FESEM) analysis.

FESEM used to validate morphology and size of Mgo particles and well distributed and spherical shaped Mgo nanoparticles generated by L. *acidophilus* with a size between (13.67- 38.86 nm) the size average of it 26.3 nm figure (3-4).

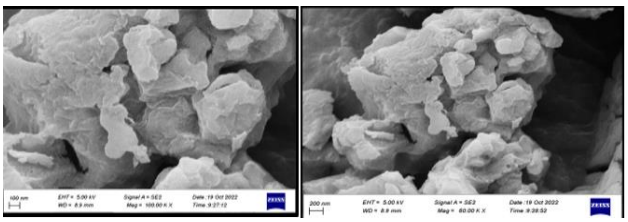

Figure (3-4): FESEM Micrograph of biogenic Mgo nanoparticle synthesized by

L. acidophilus showed MgoNPs with spherical well scattered with a size average of 26.3 nm. A: at 100 nm B: at 200 nm

Energy dispersive X-Ray spectroscopy (EDS) analysis

The optical absorption peaks of elements were observed using Energy Dispersive Spectroscopy (point and mapping analysis) to quantify the presence of Mgo NPs. The weight percentages of Mgo NPs fabricated by synthesized by L. acidophilus was 50.06 % oxygen, magnesium 10.88 % , phosphor 12.03 % , carbon 6.75 % , and potassium 0.27 %, as seen in figure (3-5) .

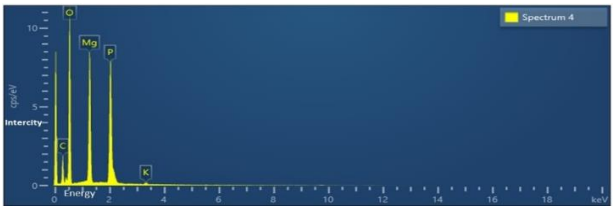

Figure (3-5) EDS analysis of Mgo NPs synthesized by L. acidophilus.

Atomic Force Microscope AFM

Atomic force microscopy (AFM) image of Mgo nanoparticle synthesis by L. acidophilus , Although the lateral dimensions are influenced by the shape of the probe, the morphology of Mgo NPs was reported. The height measurements be able to provide the elevation of nanoparticles with a high point of precision and accuracy. the average diameter of Mgo NPs biosynthesis from L. acidophilus was 9.83nm figure (3-6) which showed three dimension images, and granularity accumulation distribution charts of Mgo NPs .

Atomic Force Microscopy's extraordinary resolution allows for precise three-dimensional visualization of molecular structures, as well as atomic-scale strategies. The procedure for preparing samples for AFM is straightforward. Because samples can be viewed under near-physiological conditions, AFM can record the critical procedures of molecules, organelles, and other structures in living cells in real time(11).

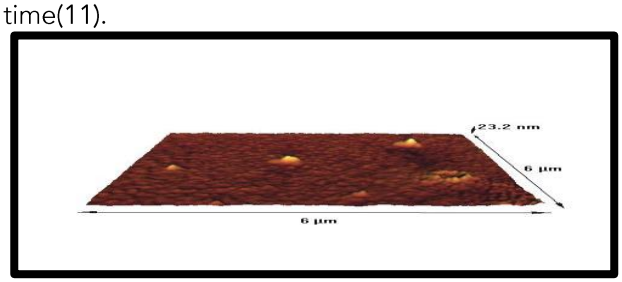

Figure (3-6) AFM analysis of biogenic Mgo synthesis by L. acidophilus X-Ray diffraction analysis (XRD)

The cubic crystal system of the synthesized MgO was confirmed by the XRD. The 2θ peak positions were well identified with the JCPDS NO: 01-076-1363. Also, the crystalline size was evaluated by the following Debye Scherrer's formula D = 0.94λ/β cosθ. (12). The strong peak suggested the inclusion of bioorganic coupons/proteins in the nanoprticles throughout the manufacturing process (Figure 3-7).

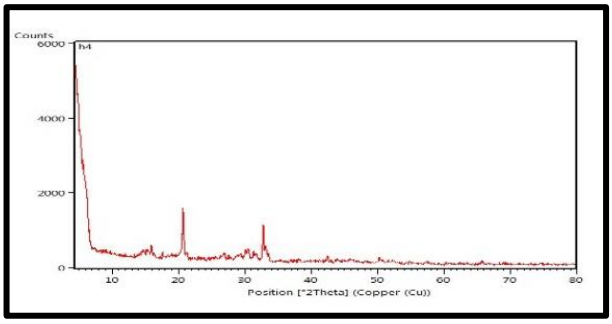

Figure (3-7): XRD analysis of Mgo nanoparticles synthesized by L. acidophilus showing the structure and size.

Antibacterial effects of Mgo nanoparticles and antibiotics

The antibacterial activity of biogenic Mgo NPs generated by *L. acidophilus* against certain Extensive drug resistance (XDR) bacterial pathogens has been tested. The bactericidal activity of biogenic Mgo NPs was determined using the agar well diffusion technique (13).

All of microorganisms studied were inhibited by Mgo NPs at different doses (200, 100 and 50 µg /ml). In Gram negative, the largest inhibition zone of Mgo NPs was (22 mm) in *P. aeruginosa*1 at a concentration of (200 µg /ml) . As the quantities of Mgo NPs were raised, the inhibitory impact became stronger. As seen in (Figure3-8) and table (3-1) . It was comparable to earlier studies that found that high concentrations of Mgo NPs inhibited bacterial growth. (14). The findings revealed that nanoparticles can limit bacterial growth in both Gram- positive and Gram-negative bacteria. Gram-negative bacteria were more sensitive to biogenic Mgo NPs than Gram- positive bacteria.

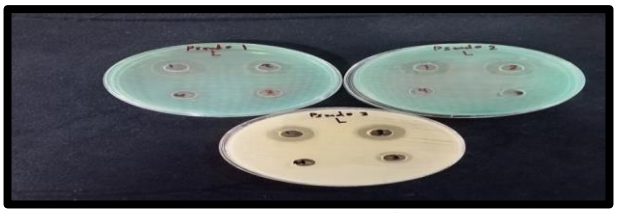

Figure (3-8) Antibacterial activity of Mgo NPs synthesis by L. acidophilus against: Three strain from P. aeruginosa

Table (3-1) – Inhibition zone of Mgo NPs synthesized by L .acidophilus against three strain from P. aeruginosa.

Tested bacteria	inhibition zone (mm)		
	50 µg/ml	100 µg/ml	200µg/ml
P. aeruginosa 1	12	18	22
P. aeruginosa 2	4	20	20
P. aeruginosa 3	13	17	18

Antibacterial action against many bacteria, including Gram-positive, Gram-negative, aerobic, and anaerobic organism, has been demonstrated. Because these proteins have no harmful impact on humans, they are excellent antibiotic substitutes (15). Current study might suggest that using probiotics that can be a solution to many problems of pathogen antibiotics resistances and can be associated with other options. Which claimed that probiotics are a double-edged sword having both good effects and related hazards, even though probiotics are now considered safe (16). The scientific community has made it their aim to create a successful alternative to replace current antibiotics that have become resistant regions, as well as an effective new entry drug complement to antibiotics, because of the mounting problem of Extensive drug resistance (XDR). Nanoparticles are now being welcomed as a possible alternative to antibiotics, with the potential to solve the bacterial XDR problem (17).

In Gram-negative bacteria like *P. aeruginosa*, as well as Gram-positive bacteria like S. aureus, Mgo NPs is reported to also have antibacterial properties (18). Mgo NPs were shown to be efficient antimicrobial medicines against a wide range of clinically relevant infections. It has been shown that the fundamental mechanism of its antibacterial action is attacking an outer membrane protein called lipopolysaccharide (LPS), which damages cell membranes and causes bacteria to die at neutral PH (19).

Anti-biofilm effect of Bioactive Mgo NPs

Biofilm seems to be the most essential property of bacteria that improves bacterium adhesion to medical equipment and prosthesis surfaces. The antibiofilm efficacy of Mgo NPs generated by *L. acidophilus* was investigated using micro titter plate technique with varied doses of Mgo NPs (512 µg /ml, 256µg/ml, 128 µg /ml, 64 µg /ml, 32 µg /ml, 16 µg /ml, 8 µg /ml, 4 µg /ml) versus three bacteria strains *P. aeruginosa* such as Gram-negative bacteria .

The antibiofilm effectiveness results differ depending on the harmful bacteria. the concentration level of Mgo NPs synthesized by *L. acidophilus* bioactive Mgo showed significant antibiofilm action, at concentration of (512 µg /ml, 256 µg /ml ,128 µg /ml, 64 µg /ml, 32 µg /ml, 16 µg /ml and 8 µg /ml). The absorption will rise from (99 to 13 %) for *P. aeruginosa* 1, (98 to 26 %) for *P. aeruginosa* 2, (99 to 12 %) *P. aeruginosa* 3 as seen in figure (3-9).

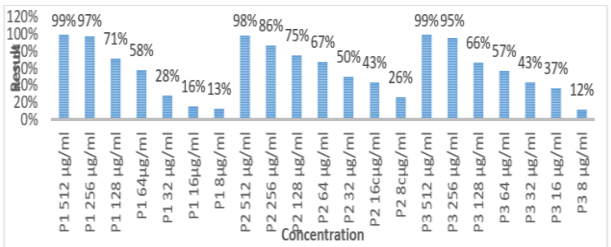

Figure (3-9): Anti-biofilm effect of Mgo NPs synthesized by L. acidophilus against pathogenic bacteria P. aeruginosa

Antioxidant activity of Mgo nanoparticles

The DPPH which is (1-Diphenyl-2-picrylhydrazyl), The free radical rummaging experiment performed to determine the antioxidant capacity of MgoNPs metabolites produced from *L. acidophilus* in vitro by decreasing DPPH free radicals. After 30 minutes of introducing nanoparticles at concentrations (1000, 500, 250, and 125 µg/ml) to the DPPH solution, the absorbance at 517 nm was determined. The capacity of nanoparticles to scavenge DPPH free radicals was demonstrated by measuring the color changes (20) . DPPH reducing the activity of nanoparticles increased with the elevation in the concentration of biogenic Mgo NPs synthesized by *L. acidophilus*. It was 84.4% in 1000 µg /ml, 82.9% in 500 µg/ ml, 81% in 250 µg /ml, and 78.5% in 125 µg/ml for Mgo NPs, Figure (3-10).

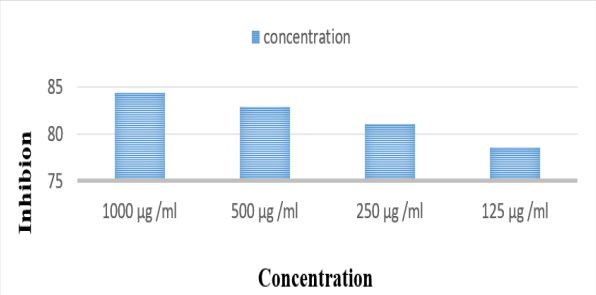

Figure (3-10): Antioxidant effect of Mgo NPs synthesized by L. acidophilus in DPPH test.

Traditionally, the antioxidant free radical rummaging capacities of a single 1-diphenyl-2-picrylhydrazyl have been calculated in vitro (DPPH). DPPH appears to be a more stable and well-known free radical, as it is reliant on reducing donor hydrogen or electron absorption. The colour change was used to study the efficacy of antioxidants to reduce DPPH (21).

The DPPH rummaging effect of nanoparticles increased as their concentration fell, showing that as the concentration of Mgo NPs decreased, the proportion of DPPH inhibition rise, and that DPPH was inhibited more due to increasing electron donation.

Antioxidants work by searching free radicals and inhibiting their formation. On oxidative stress, free radicals have a strong bactericidal action. Not only has the membrane been destroyed, but biological macromolecules such as proteins, lipids, DNA enzymes, and RNA that trigger cell death have also been harmed (22).

The effect of Mgo nanoparticles on hemolysis

Hemolysis is a condition in which red blood cells (RBCs) burst and their components are released, resulting in anemia, jaundice, and renal failure. Because all materials entering the blood come into touch with RBCs, it's critical to assess the materials' hemolytic capacity (23).

The hemolysis was identified using Triton X-100 as a positive control indicator. A sterilized phosphate buffer saline solution was employed as a negative control that allowed the stock solution to be stored at room temperature.

Mgo NPS throughout all the concentrations (1000, 500, 250, and 125 µg/ml) did not caused hemolysis in the entire blood samples examined as seen in table (3-2) This discovery is with agreement of , who found hemolysis did not caused by NPs or solvents in NPs or polymer.(27)

Table (3-2) Mgo NPs synthesized by *L. acidophilus* effect on hemolysis	
Sample	Hemolysis %
Triton X-100 (positive control)	100
PBS(negative control)	0
Blood with MgoNPs 1000 µg/ml	0
Blood with MgoNPs 500 µg/ml	0
Blood with MgoNPs 250 µg/ml	0
Blood with MgoNPs 125 µg/ml	0

References

1- Ali, A. (2018). Antimicrobial resistance pattern of uropathogens isolated from Rafha central hospital, Rafha, Kingdom of Saudi Arabia. *Journal of Pure and Applied Microbiology*, *12*(2), 577–586.

2- MacFaddin, J. F. (2000). Individual biochemical tests. *Biochemical Tests for Identification of Medical Bacteria*, 3–453.

3- Tang, Z.-X., & Lv, B.-F. (2014). MgO nanoparticles as antibacterial agent: preparation and activity. *Brazilian Journal of Chemical Engineering*, *31*, 591–601.

4- Dizaj, S. M., Lotfipour, F., Barzegar-Jalali, M., Zarrintan, M. H., & Adibkia, K. (2014). Antimicrobial activity of the metals and metal oxide nanoparticles. *Materials Science and Engineering: C*, *44*, 278–284.

5- Nguyen, N.-Y. T., Grelling, N., Wetteland, C. L., Rosario, R., & Liu, H. (2018). Antimicrobial activities and mechanisms of magnesium oxide nanoparticles (nMgO) against pathogenic bacteria, yeasts, and biofilms. *Scientific Reports*, *8*(1), 1–23.

6- Goyal, R. K. (2017). *Nanomaterials and nanocomposites: synthesis, properties, characterization techniques, and applications*.

7- Ghazi, A. A., El-Nahrawy, S., El-Ramady, H., & Ling, W. (2022). Biosynthesis of Nano-Selenium and Its Impact on Germination of Wheat under Salt Stress for Sustainable Production. *Sustainability*, *14*(3), 1784.

8- Ali, Z. H., & Aldujaili, N. H. (2022). aTherapeutic activity of Bacillus subtilis against some multidrug resistance bacteril pathogens isolated from burn infections. *AIP Conference Proceedings*, *2386*(1), 20010.

9- Shen, M., Liu, W., Zeb, A., Lian, J., Wu, J., & Lin, M. (2022). Bioaccumulation and phytotoxicity of ZnO nanoparticles in soil-grown Brassica chinensis L. and potential risks. *Journal of Environmental Management*, *306*, 114454.

10- Abd El-Hack, M. E., El-Saadony, M. T., Salem, H. M., El-Tahan, A. M., Soliman, M. M., Youssef, G. B. A., Taha, A. E., Soliman, S. M., Ahmed, A. E., & El-Kott, A. F. (2022). Alternatives to antibiotics for

organic poultry production: types, modes of action and impacts on bird's health and production. *Poultry Science*, 101696.
11- Deng, X., Xiong, F., Li, X., Xiang, B., Li, Z., Wu, X., Guo, C., Li, X., Li, Y., & Li, G. (2018). Application of atomic force microscopy in cancer research. *Journal of Nanobiotechnology*, *16*(1), 1–15.
12- Khandsuren, B., & Prokisch, J. (2021). Preparation of red and grey elemental selenium for food fortification. *Acta Alimentaria*, *50*(2), 289-298.
13- Alvi, G. B., Iqbal, M. S., Ghaith, M. M. S., Haseeb, A., Ahmed, B., & Qadir, M. I. (2021). Biogenic selenium nanoparticles (SeNPs) from citrus fruit have anti-bacterial activities. *Scientific Reports*, *11*(1), 1–11.
14- Huang, T., Holden, J. A., Heath, D. E., O'Brien-Simpson, N. M., & O'Connor, A. J. (2019). Engineering highly effective antimicrobial selenium nanoparticles through control of particle size. *Nanoscale*, *11*(31), 14937–14951.
15- Lu, J., Wu, J., Zhang, C., Zhang, Y., Lin, Y., & Luo, Y. (2018). Occurrence, distribution, and ecological-health risks of selected antibiotics in coastal waters along the coastline of China. *Science of the Total Environment*, *644*, 1469–1476.
16- Tazehabadi, M. H., Algburi, A., Popov, I. V, Ermakov, A. M., Chistyakov, V. A., Prazdnova, E. V, Weeks, R., & Chikindas, M. L. (2021). Probiotic bacilli inhibit salmonella biofilm formation without killing planktonic cells. *Frontiers in Microbiology*, *12*, 615328.
17- Morone, M. V., Dell'Annunziata, F., Giugliano, R., Chianese, A., De Filippis, A., Rinaldi, L., Gambardella, U., Franci, G., Galdiero, M., & Morone, A. (2022). Pulsed laser ablation of magnetic nanoparticles as a novel antibacterial strategy against gram positive bacteria. *Applied Surface Science Advances*, *7*, 100213.
18- Yang, X., Yu, Y., Xu, J., Shu, H., Liu, H., Wu, Y., Zhang, L., Yu, Z., Fang, M., & Yu, T. (2020). Clinical course and outcomes of critically ill patients with SARS-CoV-2 pneumonia in Wuhan, China: a single-centered, retrospective, observational study. *The Lancet Respiratory Medicine*, *8*(5), 475–481.
19- Medina Cruz, D., Mi, G., & Webster, T. J. (2018). Synthesis and characterization of biogenic selenium nanoparticles with antimicrobial properties made by Staphylococcus aureus, methicillin-resistant Staphylococcus aureus (MRSA), Escherichia coli, and Pseudomonas aeruginosa. *Journal of Biomedical Materials Research Part A*, *106*(5), 1400–1412
20- Podder, S., Chanda, D., Mukhopadhyay, A. K., De, A., Das, B., Samanta, A., Hardy, J. G., & Ghosh, C. K. (2018). c. *Inorganic Chemistry*, *57*(20), 12727–12739.
21- Dawadi, S., Katuwal, S., Gupta, A., Lamichhane, U., Thapa, R., Jaisi, S., Lamichhane, G., Bhattarai, D. P., & Parajuli, N. (2021). Current research on silver nanoparticles: Synthesis, characterization, and applications. *Journal of Nanomaterials*, *2021*.
22- Peron, S., Hadi, F., Azarbani, F., & Ananda Murthy, H. C. (2021). Antimicrobial, antioxidant, anti-glycation and toxicity studies on silver nanoparticles synthesized using Rosa damascena flower extract. *Green Chemistry Letters and Reviews*, *14*(3), 519–533.
23- Swain, P., Das, R., Das, A., Padhi, S. K., Das, K. C., & Mishra, S. S. (2019). Effects of dietary zinc oxide and selenium nanoparticles on growth performance, immune responses and enzyme activity in rohu, Labeo rohita (Hamilton). *Aquaculture Nutrition*, *25*(2), 486–494.
24- Al-Msaid Hayder, L.F.and Mohammed, H. Q. (2022). Study if Some Biomarkers in Abortion Women Undergoing Intracytoplasmic Sperm Injection (Icsi) Technique. HIV Nursing, 22(2), 1738-1740.
25- khalfa, H. M., al-msaid, H. L., abood, A. H., naji, M. A., & Hussein, S. K. (2020, December). Cellular genetic expression of purinergic receptors in different organs of male rats injected with cyclophosphoamide. In AIP Conference Proceedings (Vol. 2290, No. 1, p. 020033). AIP Publishing LLC.
26- Tshabuse, F., Buthelezi, N., Folami, A. M., Donnelly, L., & Swalaha, F. M. (2022). Rapid detection of drug-resistant Escherichia coli by Vitek 2 compact system. Water SA, 48(4), 450-456.
27- Rajkumar, S., Elanthamilan, E., Wang, S. F., Chryso, H., Balan, P. V. D., & Merlin, J. P. (2022). One-Pot Green Recovery of Copper Oxide nanoparticles from Discarded Printed Circuit Boards for electrode material in Supercapacitor Application. *Resources, Conservation and Recycling*, *180*, 106180.